International Journal of Nanotechnology and Application (IJNA)
ISSN 2277-4777
Vol. 3, Issue 2, Jun 2013, 51-62

GREEN BIOSYNTHESIS OF SILVER NANOPARTICLES USING *MORINGA OLEIFERA* L. LEAF

SMARANIKA DAS[1], UMESH KUMAR PARIDA[2] & BIRENDRA KUMAR BINDHANI[3]

[1]Department of Botany, Ravenshaw Junior College, Cuttack, Odisha, India

[2,3]School of Biotechnology, KIIT University, Campus-XI, Patia, Bhubaneswar, Odisha, India

ABSTRACT

Green synthesis of noble metal nanoparticles is a greatly developing area of research. Metallic nanoparticles have received enormous attention from chemists, physicists, biologists, and engineers who wish to use them for the development of a new-generation of nano devices. In this study, silver nanoparticles were biosynthesized from aqueous silver nitrate through a simple and eco-friendly route using *Moringa oleifera* leaf extracts, which acted as a reductant and stabilizer simultaneously. Characterizations of nanoparticles were done using different methods, which included ultraviolet-visible spectroscopy, powder X-ray diffraction, transmission electron microscopy, scanning electron microscopy, energy-dispersive X-ray fluorescence spectrometry and Fourier-transform infrared spectroscopy. The ultraviolet-visible spectrum of the aqueous medium containing silver nanoparticles showed an absorption peak at around 415 nm. Transmission electron microscopy showed that mean diameter and standard deviation for the formation of silver nanoparticles was 40-50 nm. Powder X-ray diffraction showed that the particles are crystalline in nature, with a face-centred cubic structure. The most needed outcome of this work will be the development of value-added products from *Moringa oleifera* for biomedical and nanotechnology-based industries. Furthermore, the antimicrobial potential of AgNPs was systematically evaluated. The synthesized AgNPs could competently inhibit different pathogenic organisms, including bacteria and fungi. The present research opens a new avenue for the green synthesis of nano-materials.

KEYWORDS: Silver Nanoparticles (AgNPs), *Moringa oleifera* L., Biosynthesis, Green Synthesis

INTRODUCTION

Green nanotechnology is an area with significant focus at present on the important objective of facilitating the manufacture of nanotechnology-based products that are eco-friendly and safer for all beings, with sustainable commercial viability. The “green synthesis” of metal nanoparticles receives great attention due to their unusual optical, chemical, photochemical, and electronic properties [1]. Metal nanoparticles, especially the noble metals, have mainly been studied because of their strong optical absorption in the visible region caused by the collective excitation of free-electron gas [2].

Among noble metal nanoparticles, silver nanoparticles (Ag-NPs) have a wide area of interest, as they have a large number of applications, such as in nonlinear optics, spectrally selective coating for solar energy absorption, biolabeling, intercalation materials for electrical batteries as optical receptors, catalyst in chemical reactions, and as antibacterial capacities.

The biosynthesis of nanoparticles, which represents a connection between biotechnology and nanotechnology, has received increasing consideration due to the growing need to develop environmentally friendly technologies for material syntheses. The search for appropriate biomaterials for the biosynthesis of nanoparticles continues through many different synthetic methods [3].

Today, biosynthesis of SNPs using plants or plant extracts, although biosynthesis of silver nanoparticles by plants such as *Solanum xanthocarpum L. Berry* [4], *tea leaf* [5], *Callicarpa maingayi* stem bark [6] *Bauhinia variegata* [7], *Terminalia chebula* [8], *Trachyspermum ammi and Papaver somniferum*. [9], *Hevea brasiliensis* [10], *Memecylon edule* [11], *Aloe vera* [12] have been reported, the potential of the plants as biological materials for the synthesis of nanoparticles is yet to be fully explored. *Moringa oleifera* L., a wild herbaceous plant is very common in all tropical countries, including India. The stems are slender and often reddish in color, covered with yellowish bristly hairs especially in the younger parts. The leaves are oppositely arranged, lanceolate and are usually greenish or reddish; underneath measuring about 5 cm long *Moringa oleifera* (Moringaceae) is a small to medium evergreen tree widely distributed in Asia, Africa, and America. The plant is not only well known for high nutritional contents but also recognized for its therapeutic values [13]. The leaves of *M. oleifera* have been indigenously used for various medicinal purposes such as treating bronchitis, controlling glucose level, and reducing glandular swelling [14, 15]. Numerous pharmacological investigations of *M. oleifera* leaves have been reported on anti-inflammation, anti-infection, antidiabetic, antioxidant, and antihyperlipidemic activities [16 - 21]. Recently, isoquercetin, astragalin, and crypto-chlorogenic acid were reported to be major active components in *M. oleifera* leaves [22]. Isoquercetin is a powerful natural antioxidant which possesses several potential therapeutic effects including antiasthma and antihypertension [23-25]. Astragalin is also reported as a natural antioxidant agent exhibiting some biological properties such as attenuation of inflammation, inhibition of dermatitis, and cellular protective effect [26, 27]. Chlorogenic acid and its isomers are esters of quinic and caffeic acids that have abilities to inhibit oxidation and also promote various pharmacological activities such as antiobesity, reduction of plasma and liver lipids, and inhibition of acute lung injury [28]. Standardization of herbal extracts is essential to ensure their quality and biological activities. Some analytical techniques including high performance liquid chromatography (HPLC) and liquid chromatography-mass spectrometry (LCMS) were previously developed for the quantitative analysis of the *M. oleifera* leaf extract [29]. However, a simple, rapid, and inexpensive method for routine analysis of major active constituents in the plant is still preferred. Thin-layerchromatography (TLC) densitometry is one of the suitable methods popularly used for quality control of botanical extracts because of its fast data acquisition, simplicity, and reliability [30-33]. Moreover, there has been no report on simultaneous quantification of isoquercetin, astragalin and crypto-chlorogenic acid in *M. oleifera* leaf extracts by this method before. Thus, the objectives of this work were to develop and validate a TLC-densitometric method for quantitative analysis of these principle constituents in the extracts of *M. oleifera* leaves collected from different locations in Odisha and to find good sources of this plant's raw material for pharmaceutical and nutraceutical development.

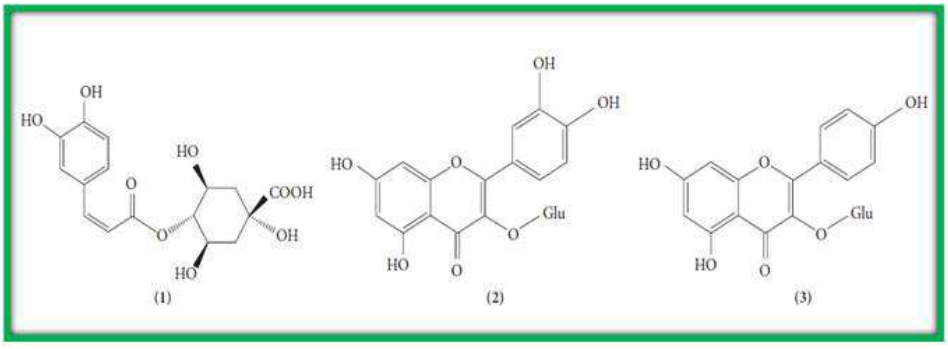

Figure 1: Chemical Structures of Crypto-Chlorogenic Acid (1), Isoquercetin (2) and Astragalin (3)

MATERIALS AND METHODS

Materials

The *M. oleifera* plants were purchased from Regional Plant Research Centre (RPRC) Bhubaneswar, Odisha, India. $AgNO_3$ (99.98%) was used as a silver precursor, and was provided by Merck (Darmstadt, Germany). HNO_3 (70%)

and HCl (37%) were obtained from Sigma-Aldrich (St Louis, MO). All reagents in this effort were analytical grade and were used as received without further purification. All solutions were freshly prepared using double-distilled water and kept in the dark to avoid any photochemical reactions. All glassware used in experimental procedures was cleaned in a fresh solution of HNO_3 / HCl (3:1, v/v), washed thoroughly with double-distilled water, and dried before use.

Plant Material Collection

Moringa oleifera L. leaves [Figure 2 A] were collected from Regional Plant Research Centre (RPRC) Bhubaneswar, Odisha India. The leaves were air dried for 10 days, and then kept in the hot air oven at 60^0C for 24 to 48 h. The leaves were ground to a fine powder.

Solvent Extraction

Ten grams of air dried powder was placed in 100 ml of organic solvent (90% methanol) in a conical flask, plugged with cotton and then kept on a rotary shaker at 180 to 200 rpm for 24 hr. After 24 hr., it was filtered through 4 layers of muslin cloth and centrifuged at 5000 × g for 10 min. The supernatant was collected and the solvent was evaporated. The crude extract diluted with 5% of DMSO to make the final volume one-tenth of the original volume and stored at 4^0C in air tight bottles for further studies [Figure 2 B].

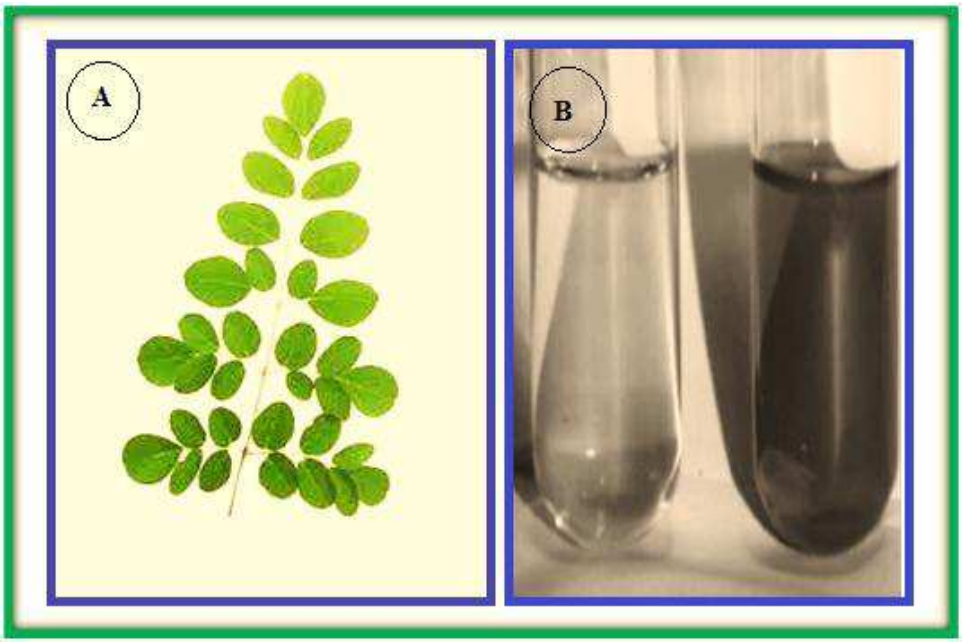

Figure 2: A. Photograph of *Moringa oleifera* and B. Silver / *Moringa oleifera* Emulsions after 24 Hours of Stirring Time. Colour Change in Reaction Mixture (Silver Nitrate and *Moringa oleifera*)

Synthesis of Ag / *M. oleifera* Emulsion

Briefly, water extract of *M. oleifera* leaves (0.1 g) was added to distilled deionized water (20 mL) with vigorous stirring for 4 hours. Forty milliliters of $AgNO_3$ (1 × 10−3 M) was then added and mixed at room temperature (25°C) for 24 hours. Ag-NPs were gradually obtained during the incubation period. Throughout the reduction process, the solution was kept at a room temperature in the dark to avoid any photochemical reactions. The solution component was purged with nitrogen gas prior to use. Subsequently, reduction proceeded in the presence of nitrogen to eliminate oxygen. The obtained colloidal suspensions of Ag/ *M. oleifera* were then centrifuged at 15,000 rpm for 20 minutes and washed four times to remove silver ion residue. The precipitate nanoparticles were then dried overnight at 30°C under vacuum to obtain the Ag/ *M. Oleifera*.

MEASUREMENTS

UV-Vis Spectroscopy

Ultraviolet-visible spectroscopy (UV-1601 pc shimadzu spectrophotometer) or ultraviolet-Visible spectrophotometer (UV-Vis) refers to absorption spectroscopy in the UV-Visible spectral region. This means it uses light in the visible and adjacent near-UV and near-infrared (NIR)) ranges. The absorption in the visible range directly affects the perceived color of the chemicals involved. In this region of the electromagnetic spectrum, molecules undergo electronic transitions.

X-Ray Diffraction (XRD) Measurements

The phase formation of bioreduced silver nanoparticles was studied with the help of XRD. The diffraction data of thoroughly dried thin films of nanoparticles on glass slides was recorded on D 8 Advanced Brucker X-ray diffractometer with Cu Kα (1.54 A^o) source.

Fourier Transmission Infra Red Spectroscopy (FTIR)

The FTIR spectrum of *O. sanctum* L. extract, $AgNO_3$ nanoparticle and amine functionalized Ag nanoparticle were recorded using were obtained using a BIORAD-FTS-7PC type FTIR spectrophotometer.

Scanning Electron Microscope (SEM) Analysis

Scanning Electron Microscope (SEM) analysis was done using Hitachi S - 4500 SEM machine. Thin films of the sample were prepared on a carbon coated copper grid by just dropping a very small amount of the sample on the grid, extra solution was removed using a blotting paper and then the film on the SEM grid were allowed to dry by putting it under a mercury lamp for 5 min.

Transmission Electron Microscope (TEM) Analysis

Transmission electron microscope (TEM) (Philips CM-10) is a microscopy technique whereby a beam of electrons is transmitted through an ultra-thin specimen, interacting with the specimen as it passes through. An image was formed from the interaction of the electrons transmitted through the specimen; the image was magnified and focused onto an imaging device.

TEST MICROORGANISMS

Antibacterial Activity

The bacterial strains studied were *Escherichia coli* (ATCC 25922), *Klebsiella pneumonia* (ATCC 15380), *Enterococcus faecalis* (ATCC 10741), *Enterobacter cloacae* (ATCC 10699), and *Proteus vulgaris* (ATCC 12454) *Staphylococcus aureus* (ATCC 25923), *Staphylococcus saprophyticus* (ATCC 35552). All microorganisms were maintained at 4°C and were obtained from Department of Botany, Berhampur University, Odisha, India.

Antimicrobial Susceptibility Test

The disc diffusion method was used to screen the antimicrobial activity. *In vitro* antimicrobial activity was screened by using Mueller Hinton Agar (MHA) obtained from Himedia (Mumbai). The MHA plates were prepared by pouring 15 ml of molten media into sterile Petri plates. The plates were allowed to solidify for 5 min and 0.1% inoculums (0.5 McFarland standards) suspension was swabbed uniformly and the inoculums was allowed to dry for 5 min. 50 µl concentration of test extract was loaded on 0.5 cm sterile disc. The loaded disc was placed on the surface of medium and the compound was allowed to diffuse for 5 min and the plates were kept for incubation at 37°C for 24 hr. At the end of

incubation, inhibition zones formed around the disc were measured with transparent ruler in millimeter. For each bacterial strain, negative controls were maintained where pure solvents were used instead of the extract. The control zones were subtracted from the test zones and the resulting zone diameter and the result obtained was tabulated. For positive control, three antibiotics, namely Cefotaxime (30 mcg/disc), streptomycin (10 mcg/disc) and Ampicillin (10 mcg/disc) were used. These studies were performed in triplicate.

RESULTS AND DISCUSSIONS

The reduction of Ag+ into Ag-NPs during exposure to water extract of *Moringa oleifera* leaf extract was able to be followed by the color change. The fresh suspension of *Moringa oleifera* was green. However, after the addition of $AgNO_3$ and stirring for 24 hours at room temperature, the emulsion turned brown.

The color changes in aqueous solutions are due to the surface-plasmon resonance (SPR) phenomenon (Figure 2 A and B). The result obtained in this investigation is interesting because it can serve as a foundation in terms of identification of potential forest plants for synthesizing Ag-NPs. *Moringa oleifera* as an aldehyde can reduce silver ions to Ag- NPs. The possible chemical equations for preparing the Ag-NPs are: After dispersion of silver ions in the *Moringa oleifera* aqueous solution matrix (Equation 1), the extract was reacted with the Ag+ (aq) to form [Ag (*M. oleifera*)] + complex, which reacted with aldehyde groups in the molecular structure of the methanolic extract to form [Ag (*M. oleifera*)], due to the reduction of silver ions through the oxidation of aldehyde to carboxylic acid groups.

UV-Visible Spectroscopy Analysis

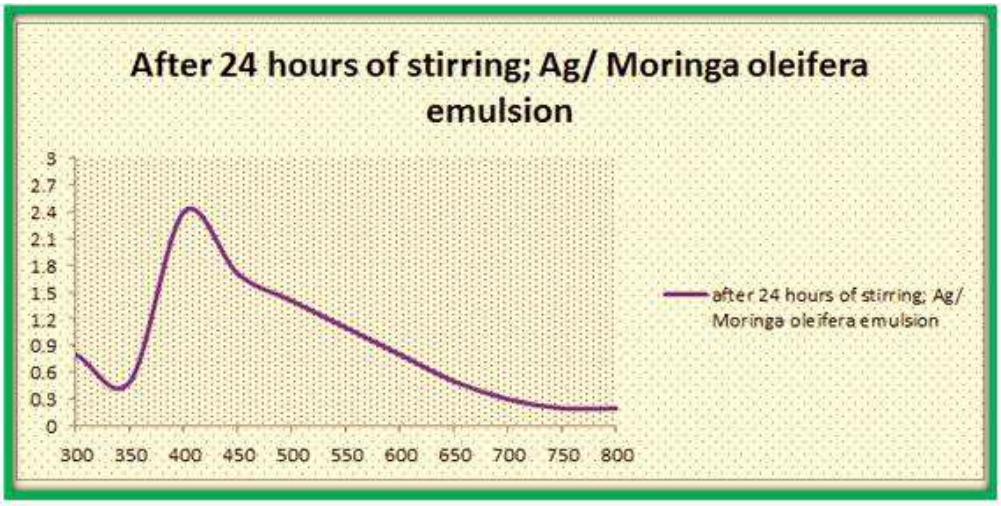

Figure 3: **UV-Visible Absorption Spectra of Silver (Ag) / *Moringa oleifera* Emulsion after 24 Hours of Stirring**

The formation of Ag-NPs was followed by measuring the SPR of the *Moringa oleifera* and Ag/ *Moringa oleifera* emulsions over the wavelength range of 300–800 nm (Figure 3). The SPR bands are influenced by the size, shape, morphology, composition, and dielectric environment of the prepared nanoparticles. Previous studies have shown that the spherical Ag-NPs contribute to the absorption bands at around 400–420 nm in the UV-visible spectra [34, 35]. These absorption bands were assumed to correspond to the Ag-NPs' extra-fine nature, with relatively small size. UV-visible absorption spectra (Figure 3) showed that the broad SPR band contained one peak at 415 nm. This peak illustrates the presence of a homogeneous distribution of hydrosol Ag-NPs after 24 hours stirring. For the stability test of the Ag-NP emulsion, the absorption spectrum of the sample was measured after storage for 3 months (Figure 3). The absorption peak of the Ag-NPs shifted slightly from 415 to 417 nm, but the spectra for these two samples showed significant changes in either peak intensity or spectral shape [35]. Thus, it can be concluded that for emulsion stability testing, due to the

decreases in absorbance intensity and deposits of Ag-NPs, at first the stability of the Ag / *Moringa oleifera*. longa emulsion decreases and then gradually the size of the Ag-NPs increases.

Powder X-Ray Diffraction

Figure 4 shows the *Moringa oleifera* extract-mediated synthesized Ag nanostructure was confirmed by the characteristic peaks observed in the XRD image. All diffraction diffraction lines observed at 2θ angle 37.59°, 44.29°, 64.68°, and 76.98° respectively, have been indexed as (111), (200), (220) and (311) respectively. XRD patterns were analyzed to determine peak intensity, position and width, full-width at half-maximum (FWHM) data was used with the Scherer formula explained in section materials and method. The average particle size of Ag-NPs can be calculated using the Debye–Scherrer equation: where K is the Scherrer constant with value from 0.9 to 1 (shape factor), where λ is the X-ray wavelength (1.5418 Å), β½ is the width of the XRD peak at half-height and θ is the Bragg angle. From the Scherrer equation, the average crystallite size of Ag-NPs for the sample at 24 hours. The typical XRD pattern revealed that the sample contains a mixed phase (cubic and hexagonal) structures of silver nanoparticles. The average estimated particle size of this sample was 40-50 nm derived from the FWHM of peak corresponding to 111 planes with cubic and hexagonal shape which is also in line with the TEM results discussed later [36].

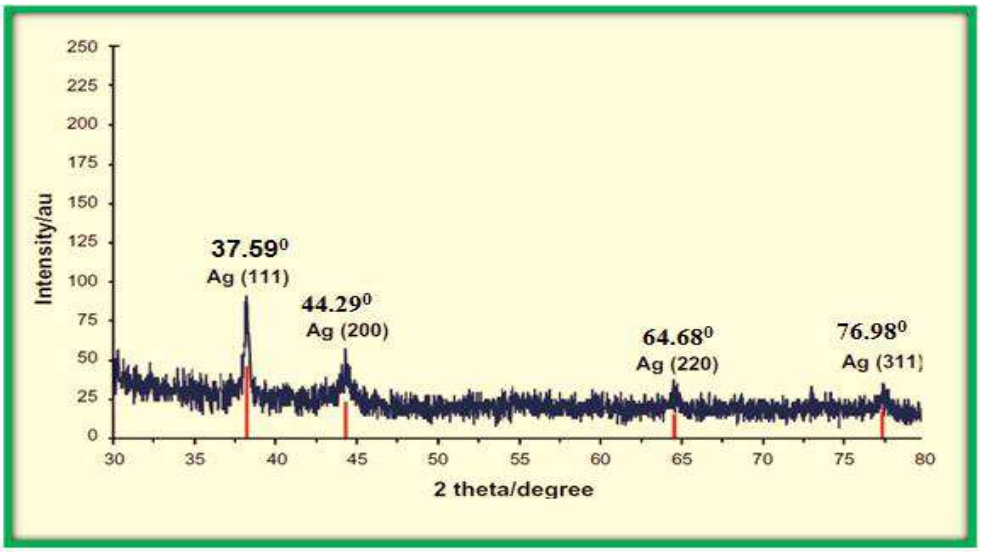

Figure 4: X-Ray Diffraction Patterns of Silver Nanoparticles (Ag-NPs) Synthesized in *Moringa oleifera* for Determination of Ag-NPs after 24 Hours of Stirring

TEM

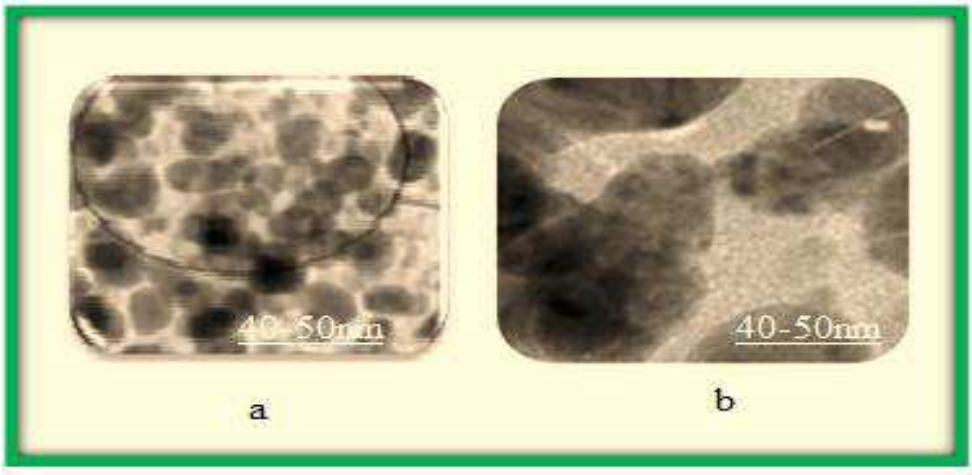

Figure 5: Transmission Electron Microscopy Images of Silver / *Moringa oleifera* after 24 Hours of Stirring

The Ag-NP solution synthesized by treating silver nitrate solution with *Moringa oleifera* was deposited onto a TEM copper grid. After drying, the grid was imaged using TEM. The TEM images and their size distribution are shown in Figure 5a and b; the result showed narrow particle-size distributions, with diameters in the range of 40-50 nm. The presence of one narrow distribution of Ag-NPs in the TEM images is in accordance with the UV-visible spectral study. Figure 5 show the Ag-NPs surrounded by the extract of *Moringa oleifera*. The dark points in this figure represent the large-scale distribution of Ag-NPs. The Ag-NPs surrounded by *Moringa oleifera* extract is shown by TEM and confirmed by FT-IR spectroscopy.

SEM

Figure 6 shows the SEM images for the *Moringa oleifera* and Ag/ *Moringa oleifera* emulsion after 24 hours stirring. These results confirm that extract of *Moringa oleifera* can effectively control the shape and size of the Ag-NPs. The exterior surfaces of Ag/ *Moringa oleifera* due to the presence of small Ag-NPs become shiny in the spots' spherical shapes (Figure 6).

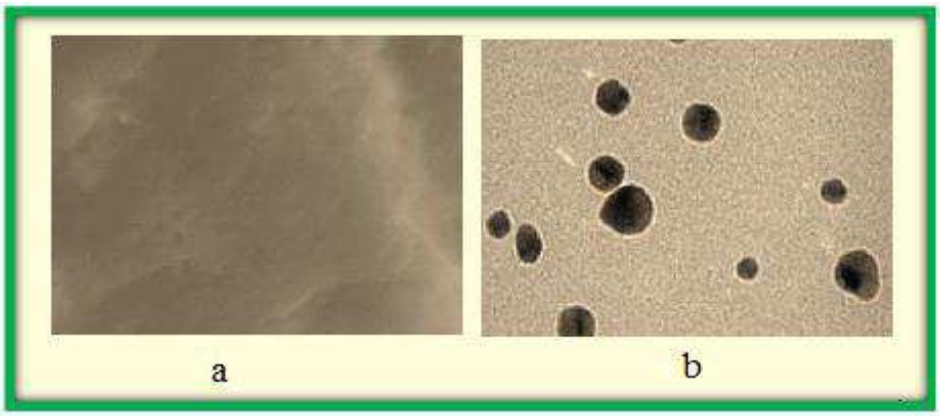

Figure 6: Scanning Electron Microscopy Image of *Moringa oleifera* (A) and Silver/ *Moringa oleifera* (B) Formation after 24 Hours of Stirring

FT-IR Chemical Analysis

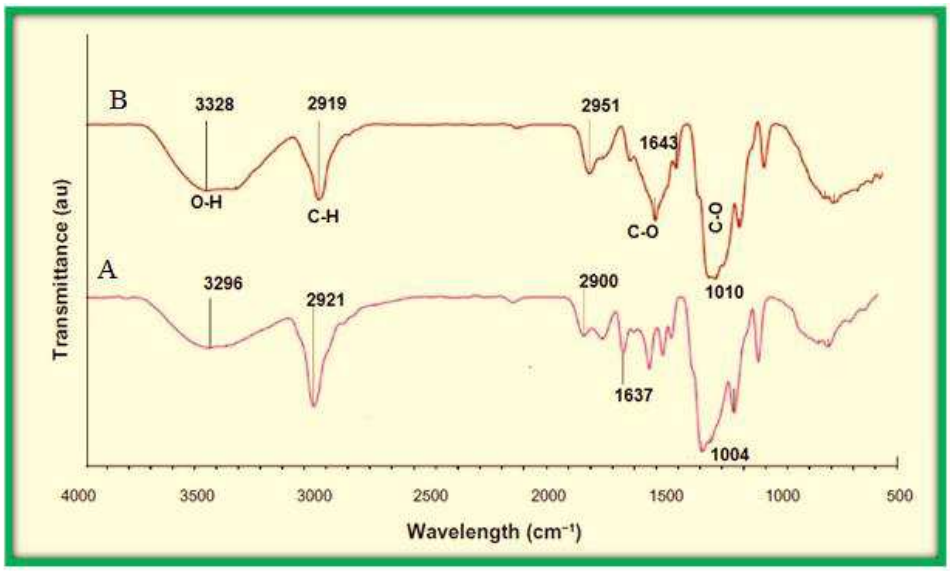

Figure 7: Fourier-Transform Infrared Spectra for the *Moringa oleifera* Leaf Extract (A) and Ag/ *Moringa oleifera* (B) after 24 Hours from Biosynthesis Reaction

The FT-IR spectra were recorded to identify the possible biomolecules responsible for the reduction of the Ag+ ions and capping of the bioreduced Ag-NPs synthesized by the *Moringa oleifera* extract. After complete bioreduction of Ag+, the *Moringa oleifera* leaf powder extract was centrifuged at 15,000 rpm for 20 minutes to isolate the Ag-NPs from

proteins and other compounds present in the solution. Figure 7A shows the FT-IR spectrum of *Moringa oleifera* leaf powder that did not contain AgNO3, whereas Figure 7B shows the spectrum containing Ag-NPs after extract bio-reduction with AgNO3. The spectrum in Figure 7A shows transmission peaks at 3296, 2921, 2900, 1637, 1004 cm^{-1}. Similarly, in Figure 7B transmission peaks for the Leaves-powder extract containing Ag-NPs were at 3328, 2919, 2951, 1643, 1010 cm^{-1}. Three absorption peaks located around 1010 can be assigned as the absorption peaks of –C–N stretching vibrations of the amine, –C–O–C or –C–O groups, respectively [37]. The bonds or functional groups such as –C–O–C–, –C–O, and –C=C– derived from heterocyclic compounds, e.g., alkaloid or flavones and the amide (I) bond derived from the proteins that are present in the leaves-powder extract are the capping ligands of the nanoparticles. The broad and strong bands at 3328–2921 cm^{-1} were due to bonded hydroxyl (–OH) or amine groups (–NH) and aliphatic C–H of the *M. oleifera* leaves-powder extract, respectively. The peak at 1643 cm^{-1} is attributed to the carboxyl group (–C=O) stretching vibration. The adsorption at around 1300–1500 cm^{-1} notably showed that $–NO_3$ existed in residual amounts [38]. The peak in 1010 and 1004cm^{-1} are related to Ag-NP banding with oxygen from hydroxyl groups of *Moringa oleifera* compounds (Figure 7B) [35].

Table 1: Antibacterial Activity of AgNPs

Microorganism	Cef	Amp	Str	Ag NP	Control
E. coli	37 ± 1.81	-	42 ± 2.12	14 ± 0.32	0.0
E. cloacae	-	-	-	16 ± 0.8	0.0
E. faecalis	-	-	28 ± 0.76	15 ± 0.06	0.0
P. vulgaris	13 ± 0.65	-	28 ± 0.66	13 ± 0.03	0.0
K. pneumoniae	-	-	27 ± 0.54	11 ± 0.05	0.0
S. aureus	26 ± 1.23	34 ± 1.43	30 ± 1.99	12.60 ± 0.90	0.0
S. saprophyticus	40 ± 1.73	42 ± 2.21	46 ± 2.07	12.10 ± 0.02	0.0

The results for antibacterial activity of silver nanoparticless were shown in Table -1. The most potent effect, related to methanol extract of *Moringa oleifera* L. showed inhibition effect against *S. aureus* as well as *S. saprophyticus* in similar degree of inhibition zone diameter (12.60 ± 0.90 and 12.10 ± 0.02). MIC values for the active extract are indicated in Table- 1. Inhibition zone values were obtained from the synthesized silver nanoparticle suspension and were tested against *E. coli*, *E. cloacae*, *K. pneumoniae*, *S. aureus,* and *E. faecalis and P. vulgaris*. The results and images of inhibition zones are presented as the average values in Table-1. It shows that the Ag NPs suspension gave high and similar antibacterial activity against Gram-negative and Gram-positive bacteria. Because of their size, Ag NPs can easily reach the nuclear content of bacteria and they present a large and impressive surface area, enabling broad contact with bacteria. This could be the reason why they gave the best antibacterial effect. For solid support systems, some researchers have argued that Ag+ ions released from the surface of Ag NPs were responsible for their antibacterial activity. For aqueous phase systems, the results show that the antibacterial test of Ag+ ions was high at the concentration levels reached by releasing, and that the presence of Ag NPs was very important, which reinforces the idea that the larger the surface area the stronger the antibacterial activity. The diameters of inhibition zone in the agar plate were given in mm. The tests were repeated three times for each treated sample, and the results were presented in Table - 1. The suspension of antibacterial activity of *E. coli* was higher than *E. cloacae* and the antibacterial activity of *K. pneumoniea* is also higher than *S. aures* [39 - 40].

CONCLUSIONS

Ag-NPs with an average size of 40-50 nm and spherical shapes were synthesized using aqueous leaf powder extract of *M. oleifera*. The Ag-NPs were characterized by UV-visible, XRD, TEM, SEM and FT-IR spectra. Biosynthesis of Ag-NPs using green resources like *is* a better alternative to chemical synthesis, since this green synthesis is pollutant-

free and eco-friendly. From the results obtained in this research, one can affirm that *M. oleifera* leaves powder can play an important role in the bioreduction and stabilization of silver ions to Ag-NPs. The antibacterial and antifungal activities of the nanoparticles have been evaluated. Our current study revealed that the minimum inhibitor concentration (MIC) of *S. saprophyticus* (12.60 ± 0.90 mg/ml) was lesser than the other test microorganisms and which was followed by *S. aureus* (12.10 ± 0.02 mg/ml). *S. saprophyticus* was an uropathogenic *staphylococcus* frequently isolated from young female outpatients with uncomplicated urinary tract infections. *S. saprophyticus* was a true urinary tract pathogen causing both upper and lower urinary tract infections. The present study emphasized the use of plant medicinal for the synthesis of silver nanoparticle with antibacterial and antifungal effect. Further studies with other plant-mediated synthesis of silver nanoparticles are in progress.

ACKNOWLEDGEMENTS

Thanks are due to Head of the Department of Botany, Ravenshaw University and also Director, School of Biotechnology, KIIT University for providing necessary laboratory facilities for this investigation. The authors are grateful to the Department of Botany, Berhampur University, Odisha for providing bacterial strains for this work. Authors also thank the Director CIPET, Bhubaneswar & Chennai for various analytical tests and encouragement.

REFERENCES

1. Mohanpuria, P., Rana, N. K.., & Yadav, S. K. (2008). Biosynthesis of nanoparticles: technological concepts and future applications. Journal Nanopart Res., 10, 507–517.
2. Mohamed, M. B., Volkov, V., Link, S., & Sayed, MAE. (2000). The ‘lightning’ gold nanorods: fluorescence enhancement of over a million compared to the gold metal. Chem Phys Lett., 317, 517–523.
3. Sathishkumar, M., Sneha, K., Won, S. W., Cho, C. W., Kim, S., & Yun, Y. S. (2009). *Cinnamon zeylanicum* bark extract and powder mediated green synthesis of nano-crystalline silver particles and its bactericidal activity. Colloid Surface B., 73, 332–338.
4. Amin, M., Anwar, F., Janjua, M. R., Iqbal, M. A., & Rashid, U. (2012). “Green Synthesis of Silver Nanoparticles through Reduction with *Solanum xanthocarpum* L. Berry Extract”: Characterization, Antimicrobial and Urease Inhibitory Activities against Helicobacter pylori. Int J Mol Sci, 13(8), 9923-41.
5. Loo, Y. Y., Chieng, B. W., Nishibuchi, M., & Radu, S. (2012). “Synthesis of silver nanoparticles by using tea leaf extract from *Camellia Sinensis*”. Int J Nanomedicine, 7, 4263-7.
6. Shameli, K., Bin Ahmad, M., Jaffar Al-Mulla, E. A., Ibrahim, N. A., Shabanzadeh, P., Rustaiyan, A., Abdollahi, Y., Bagheri, S., Abdolmohammadi, S., Usman, M. S., & Zidan, M. (2012). “Green biosynthesis of silver nanoparticles using *Callicarpa maingayi* stem bark extraction”. Molecules, 17(7), 8506-17.
7. Kumar, V., & Yadav, S. K. (2012). Synthesis of different-sized silver nanoparticles by simply varying reaction conditions with leaf extracts of *Bauhinia variegata* L. IET Nanobiotechnol, 6(1), 1-8.
8. Mohan Kumar, K.., Sinha, M., Mandal, B. K., Ghosh, A. R., Siva Kumar, K., & Sreedhara Reddy, P. (2012). Green synthesis of silver nanoparticles using *Terminalia chebula* extract at room temperature and their antimicrobial studies. Spectrochim Acta A Mol Biomol Spectrosc, 91, 228-33.
9. Vijayaraghavan, K., Nalini, S. P., Prakash, N. U., & Madhankumar, D. (2012). One step green synthesis of silver nano/microparticles using extracts of *Trachyspermum ammi* and *Papaver somniferum*. Colloids Surf B

Biointerfaces 1, 94, 114-7.

10. Guidelli, E. J., Ramos, A. P., Zaniquelli, M. E., & Baffa, O. (2011). Green synthesis of colloidal silver nanoparticles using natural rubber latex extracted from *Hevea brasiliensis*. Spectrochim Acta A Mol Biomol Spectrosc, 82(1), 140 -5.
11. Elavazhagan, T., & Arunachalam, K. D. (2011). *Memecylon edule* leaf extract mediated green synthesis of silver and gold nanoparticles. Int J Nanomedicine, 6, 1265-78.
12. Panda, S., Kar, A. 1998. *Ocimum sanctum* leaf extract in the regulation of thyroid function in the male mouse. Pharmacol. Res., 38(2), 107-110.
13. Anwar, F., Latif, S., Ashraf, M., & Gilani, A. H. (2007). *Moringa oleifera*: a food plant with multiple medicinal uses. Phytotherapy Research, 21 (1), 17–25.
14. Pandey, A., Pradheep, K., Gupta, R., Nayar, E. R., & Bhandari, D. C. (2011). Drumstick tree' (*Moringa oleifera* Lam.): a multipurpose potential species in India. Genetic Resources and Crop Evolution, 58 (3), 453–460.
15. Ou´edraogo, M., Lamien-Sanou, A., & Ramde, N. (2013). Protective effect of *Moringa oleifera* leaves against gentamicin-induced nephrotoxicity in rabbits. Experimental and Toxicologic Pathology, 65 (3) 335–339.
16. Singh, B. N., & Singhet, R. L. (2009). OxidativeDNAdamage protective activity, antioxidant and anti-quorum sensing potentials of *Moringa oleifera*. Food and Chemical Toxicology, 47 (6), 1109–1116.
17. Ndong, M., Uehara, M., Katsumata, S. I., & Suzuki K. (2007). Effects of oral administration of *Moringa oleifera* Lam on glucose tolerance in Goto-Kakizaki and wistar rats. Journal of Clinical Biochemistry and Nutrition, 40, (3), 229–233.
18. Verma, A. R., Vijayakumar, M., Mathela, C. S., & Rao, C.V. (2009). In vitro and in vivo antioxidant properties of different fractions of *Moringa oleifera* leaves. Food and Chemical Toxicology, 47 (9), 2196–2201.
19. Chumark, P., Khunawat, P. & Sanvarinda, Y. (2008). The *in vitro* and *ex vivo* antioxidant properties, hypolipidaemic and antiatherosclerotic activities of water extract of *Moringa oleifera* Lam. Leaves. Journal of Ethnopharmacology, 116 (3), 439–446.
20. Vongsak, B., Sithisarn, P., & Gritsanapan, W. (2012). HPLC quantitative analysis of three major antioxidative components of *Moringa oleifera* leaf extracts. Planta Medica, 78 (11), 1252.
21. Jung, S. H., Kim, B. J., Lee, E. H., & Osborne, N. N. (2010). Isoquercitrin is the most effective antioxidant in the plant *Thuja orientalis* and able to counteract oxidative-induced damage to a transformed cell line (RGC-5 cells). Neurochemistry International, 57 (7), 713–721.
22. Fernandez, J., Reyes, R., & Ponce, H., (2005). Isoquercitrin from *Argemone platyceras* inhibits carbachol and leukotriene D4- induced contraction in guinea-pig airways. European Journal of Pharmacology, 522 (1–3), 108–115.
23. Gasparotto, A., Gasparotto, F. M., & Lourenc¸o E. L. B. (2011). Antihypertensive effects of isoquercitrin and extracts from *Tropaeolum majus* L.: evidence for the inhibition of angiotensin converting enzyme. Journal of Ethnopharmacology, 134 (2), 363–372.

24. Park, S. N., Kim, S. Y., Lim, G. N., Jo, N. R., & Lee, M. H. (2012). *In vitro* skin permeation and cellular protective effects of flavonoids isolated from *Suaeda asparagoides* extracts. Journal of Industrial and Engineering Chemistry, 18 (2), 680– 683.

25. Soromou, L. W., Chen, N., & Jiang, L. (2012). Astragalin attenuates lipopolysaccharide-induced inflammatory responses by downregulating NF-*κ*B signaling pathway. Biochemical and Biophysical Research Communications, 419 (2), 256–261.

26. Kotani, M., Matsumoto, M., & Fujita, A. (2000). Persimmon leaf extract and astragalin inhibit development of dermatitis and IgE elevation in NC/NGa mice. Journal of Allergy and Clinical Immunology, 106 (1), 159–166.

27. Nakatani, N., Kayano, S. I., Kikuzaki, H., Sumino, K., Katagiri, K., & Mitani, T. (2000). Identification, quantitative determination, and antioxidative activities of chlorogenic acid isomers in prune (*Prunus domestica* L.). Journal of Agricultural and Food Chemistry, 48 (11), 5512–5516.

28. Cho, A. S., Jeon, S. M., & Kim, M. J. (2010). Chlorogenic acid exhibits anti-obesity property and improves lipid metabolism in high-fat diet-induced-obese mice. Food and Chemical Toxicology, 48 (3), 937–943.

29. Rodriguez de Sotillo D. V., & Hadley, M. (2002). Chlorogenic acid modifies plasma and liver concentrations of: cholesterol, triacylglycerol, and minerals in (fa/fa) Zucker rats. The Journal of Nutritional Biochemistry, 13 (12), 717–726.

30. Zhang, X., Huang, H., & Yang, T. (2010). Chlorogenic acid protects mice against lipopolysaccharide-induced acute lung injury. Injury, 41 (7), 746–752.

31. Bennett, R. N., Mellon, F. A., & Foidl, N. (2003). Profiling glucosinolates and phenolics in vegetative and reproductive tissues of the multi-purpose trees *Moringa oleifera* L. (Horseradish tree) and *Moringa stenopetala* L. Journal of Agricultural and Food Chemistry, 51 (12), 3546–3553.

32. Bodoki, E., Oprean, R., Vlase, L., Tamas, M., & Sandulescu, R. (2005). Fast determination of colchicine by TLC-densitometry from pharmaceuticals and vegetal extracts. Journal of Pharmaceutical and Biomedical Analysis, 37 (5), 971–977.

33. Cimpoiu, C., Hosu, A., Seserman, L., Sandru, M. & Miclaus, V. (2010). Simultaneous determination of methylxanthines in different types of tea by a newly developed and validated TLC method. Journal of Separation Science, 33 (23-24), 3794–3799.

34. Stepanov, A. L. (1997). Optical properties of metal nanoparticles synthesized in a polymer by ion implantation: a review. Tech Phys, 49, 143–153.

35. Shameli, K., Ahmad, M. B., & Jazayeri, S. D. (2012). Investigation of antibacterial properties silver nanoparticles prepared via green method. *Chem Cent J*. 2012; 6:73.

36. Shameli, K., Ahmad, M. B., Zamanian, A., Sangpour, P., Shabanzadeh, P., Abdollahi, Y., & Zargar, M. (2012). Green biosynthesis of silver nanoparticles using *Curcuma longa* tuber powder. International Journal of Nanomedicine, 7, 5603–5610

37. Huang, J., Li, Q., & Sun, D. (2007). Biosynthesis of silver and gold nanoparticles by novel sundried *Cinnamomum camphora* leaf. Nanotechnology, 18, 1–11.

38. Shameli, K., Ahmad, M. B., & Al-Mulla, EAJ. (2012). Green biosynthesis of silver nanoparticles using *Callicarpa maingayi* stem bark extraction. Molecules, 17, 8506–8517.

39. Shrivastava, S., Bera, T., Roy, A., Singh, G., Ramachandrarao, P., & Dash, D. (2007). Characterization of enhanced antibacterial effects of novel silver nanoparticles. Nanotechnology, 18, 225103(9pp).

40. Shahverdi, A. R., Fakhimi, A., Shahverdi, H. R., & Minaian, S. (2007). Synthesis and effect of silver nanoparticles on the antibacterial activity of different antibiotics against *Staphylococcus aureus* and *Escherichia coli.* Nanomedicine, 3, 168-171.